

# Saint-Venant torsion constant of modern precast concrete bridge girders

Richard Brice and Richard Pickings

- This paper presents methodology and results of a study to determine the torsion constant for many of the modern precast, prestressed concrete bridge girders used in the United States.
- Results are compared with values from the American Association of State Highway and Transportation Officials' *AASHTO LRFD Bridge Design Specifications* approximate methods.
- An online appendix contains an extensive catalog of geometric properties for the girder sections considered in this study.

**M**any bridge owners have developed new precast, prestressed concrete bridge girder sections that are optimized for high-performance concrete and pretensioning strands with diameters greater than 0.5 in. (12.7 mm). Girder sections have been developed for increased span capacities, while others fill a need in shorter-span ranges.<sup>1-4</sup>

Accurate geometric properties are essential for design. Common properties, including cross-sectional area, location of centroid, and major axis moment of inertia, are generally easy to compute and are readily available in standard design references. Computation of the torsion constant is a different matter. Closed-form solutions exist for a few simple shapes, such as rectangles, triangles, and ellipses, but are intractable for other shapes, making it necessary to use gross assumptions or numerical approximations. The American Association of State Highway and Transportation Officials' *AASHTO LRFD Bridge Design Specifications*<sup>5</sup> provide approximate equations for estimating this important design parameter, but these equations are based on assumptions that can lead to inaccurate results for common bridge beam sections. This paper presents the methods and results of a study to determine the torsion constant for many of the modern precast, prestressed concrete bridge girders used in the United States and compares the results with values from the approximate methods of the AASHTO LRFD specifications.

*PCI Journal* (ISSN 0887-9672) V. 66, No. 3, May–June 2021.

*PCI Journal* is published bimonthly by the Precast/Prestressed Concrete Institute, 8770 W. Bryn Mawr Ave., Suite 1150, Chicago, IL 60631.

Copyright © 2021, Precast/Prestressed Concrete Institute. The Precast/Prestressed Concrete Institute is not responsible for statements made by authors of papers in *PCI Journal*. Original manuscripts and discussion on published papers are accepted on review in accordance with the Precast/Prestressed Concrete Institute's peer-review process. No payment is offered.

## Background

Torsional rigidity relates applied torque to the angle of twist per unit length of a prismatic structural member as:<sup>6</sup>

$$\frac{\theta}{L} = \frac{T}{GJ}$$

where

$\theta$  = angle of twist

$L$  = member length

$T$  = torque

$G$  = shear modulus

$J$  = Saint-Venant torsion constant

The Saint-Venant torsion constant  $J$  is a geometric property of the cross section. The torsion constant, along with other cross-sectional properties, is frequently used in linear elastic three-dimensional finite element analysis. It is also used in the evaluation of girder stability during active construction scenarios.<sup>7</sup> A literature search for torsion constants for modern precast, prestressed concrete bridge girders did not identify published values. Torsion constants for AASHTO Type I to Type VI sections were computed and published by Eby et al.<sup>8</sup> in 1973 and then updated by Yoo<sup>9</sup> in 2000. The analysis by Eby et al. used a discretization of AASHTO Type V and Type VI girders that did not accurately represent the top flange shape, reducing accuracy for these sections. The *PCI Bridge Design Manual*<sup>10</sup> incorporates the torsion constants published by Eby et al.

## Saint-Venant torsion problem and Prandtl membrane analogy solution

The general theory of torsion commonly used in beam analyses is attributed to Saint-Venant. Computation of the torsion constant is complex and generally intractable for all but the simplest shapes. Prandtl first suggested an analogy between the differential equation of the torsion problem and the differential equation representing the surface of a thin membrane stretched across an opening having the same shape as the cross section being evaluated and slightly elevated by a small change in pressure. The torsion constant is proportional to the volume under the membrane bubble. The membrane analogy, often called the soap bubble analogy, provides a means to solve the torsion problem for irregular shapes.

Early methods to solve the Prandtl membrane analogy involved literally measuring the volume under a soap bubble. In 1958, Bonanno<sup>11</sup> constructed thin aluminum plates with the outline of irregular shapes cut out of the center, applied a soap film over the opening, and photographed the resulting soap bubble. Photogrammetry was then used to identify elevation contours from photographic plates and a planimeter was used to measure

the area enclosed by the contours. The volume under the soap bubble was subsequently computed by Simpson's rule.

Both Eby et al. and Yoo used digital computers to solve the membrane analogy problem in their studies. The computation of the volume under a virtual soap bubble based on the membrane analogy is accomplished by numerically solving the governing differential equation for the ordinates and using numerical integration to compute the resulting volume. The most common method is to discretize the cross section into a mesh of square or rectangular elements and then solve the differential equation using the finite difference method with central differences.<sup>12</sup> Each mesh element and the membrane ordinate form a parallelepiped. The volume under the membrane is found by summing the volumes of each parallelepiped under an average ordinate. **Figure 1** illustrates a finite difference mesh, the membrane bubble solution, and a typical parallelepiped for an AASHTO Type II girder.

Eby et al. and Yoo used a second-order Taylor series approximation of the governing differential equation for the finite difference analysis. Yoo notes that the approximation gives a lower-bound value for the torsion constant. This is because a portion of the volume under the membrane is neglected when using an average ordinate of a parallelepiped. The neglected volume is proportional to the area of the mesh elements. Additional error is attributed to the truncation error of the Taylor series approximation. The exact truncation error is unknown but reasonably assumed to be small because the smooth shape of the membrane suggests that higher order derivatives are insignificant. The truncation error is known to be a multiple of the square of the mesh element size.<sup>13</sup> Reducing the size of the mesh elements reduces the neglected volume and the truncation error; however, significantly more finite difference equations must be solved. Yoo provides an excellent description of the numerical solution, which will not be repeated herein. Readers are encouraged to review Yoo's presentation of the torsion problem and solution.

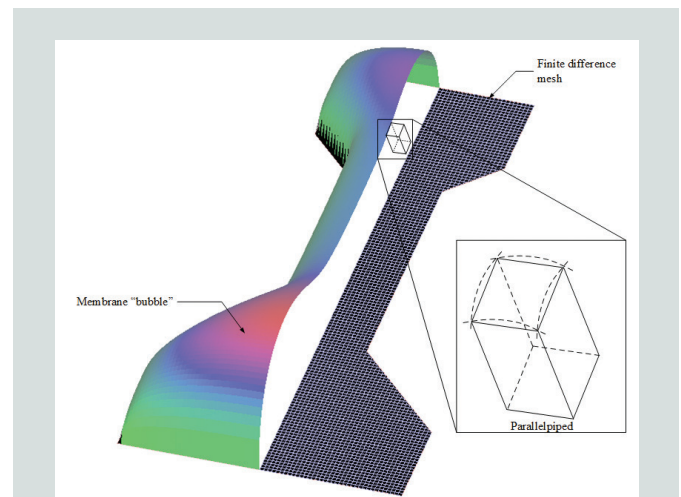


**Figure 1.** Finite difference mesh, membrane bubble solution, and typical parallelepiped for an American Association of State Highway and Transportation Officials Type II girder.

## Computational solution

Neither Eby et al. nor Yoo provided specifications for the computers used in their studies. However, we reasonably assume the computing capacity of 1973- and 2000-era digital computers limited the number of finite difference equations that could be solved, thereby limiting the accuracy of their results. Eby et al. report varying the granularity of finite difference meshes between 160 and 185 points. Yoo used a finite difference mesh with  $\frac{1}{2}$  in. (12.7 mm) square mesh elements; therefore, the number of mesh elements varied depending on the cross-sectional area of the girder evaluated. Yoo modeled the AASHTO Type II girder with approximately 700 mesh points.

Each mesh point yields a finite difference equation with the number of unknown quantities equal to the number of mesh points. A section modeled with  $N$  mesh points requires finite difference equations with an  $N \times N$  coefficient matrix and  $N$  unknowns. The number of equations can be reduced by approximately half for sections with one axis of symmetry, as is typical for precast concrete girders. Finite difference equations are not needed for exterior boundary mesh points because they represent boundary conditions with an ordinate of zero.

This study used the same finite difference method to solve the membrane analogy problem but differed in several significant ways. The accuracy of torsion constants for AASHTO Type I to Type VI girders were improved. Previously unpublished torsion constants were computed for modern precast concrete bridge girders used in various regions of the United States. The torsion constants for these modern precast concrete girders were compared with values computed with the approximation equations given in the AASHTO LRFD specifications. Computations were carried out with a new computer software program that takes advantages of modern digital computing technology, permitting a much finer finite difference mesh with significantly more computational effort to be used in an efficient manner to improve accuracy.

## Modeling

A key element in the development of the finite difference solution is the discretization of the girder cross section into a mesh. Eby et al. used mesh grids of various sizes with square and rectangular elements. Complex volume approximations were made for boundary elements to compensate for the large size of the mesh elements and poor fit with the sloped edges of the beam cross sections studied. Yoo used a simple mesh of square elements where the sloped edges of the beam cross sections were modeled in a stairstep fashion (Fig. 2). Volume errors for the boundary elements were negligible due to the small size of the mesh elements.

The same simple square element meshing scheme was used in this study; however, the size of the mesh elements was one-fourth those used by Yoo. Mesh elements that were  $\frac{1}{8}$  in.

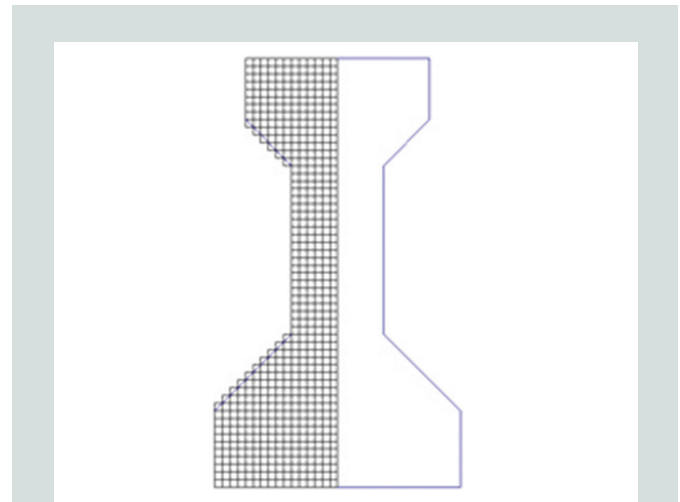


**Figure 2.** Finite difference mesh for an American Association of State Highway and Transportation Officials Type II girder using a  $\frac{1}{2}$  in. grid with sloped edges modeled in a stairstep fashion. Note: 1 in. = 25.4 mm.

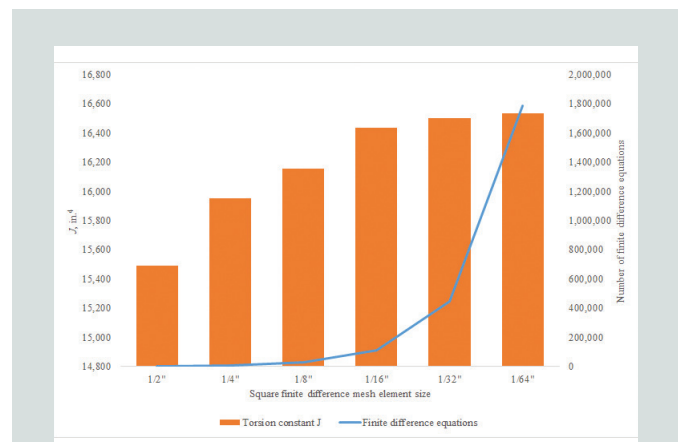


**Figure 3.** Torsion constant and number of finite difference equations used for a Washington State Department of Transportation WF66G girder section for various finite difference mesh sizes. Note: 1" = 1 in. = 25.4 mm; 1 in.<sup>4</sup> = 416,231 mm<sup>4</sup>.

(3.175 mm) square, resulting in thousands of finite difference equations per cross section, were used, yielding very accurate results. With mesh elements that were a factor of four smaller than those used by Yoo, the volume of each parallelepiped was more precise, and the Taylor series truncation error was reduced by a factor of 16. The AASHTO Type II girder was modeled with 11,676 mesh points in this study.

There is a point of diminishing returns with respect to mesh size and solution accuracy. The finite difference numerical approximation quickly converges as the size of the mesh elements reduces. Figure 3 shows the torsion constant and number of finite difference equations for a Washington State Department of Transportation WF66G girder section computed with mesh elements ranging in size from  $\frac{1}{2}$  to  $\frac{1}{64}$  in. (12.7 to 0.4 mm) square. The torsion constant with  $\frac{1}{8}$  in. (3.175 mm) square mesh elements is 4% larger than with  $\frac{1}{2}$  in. square elements. Decreasing the mesh size to  $\frac{1}{64}$  in.

square elements increases the torsion constant by 7% over the value for 1/2 in. square mesh elements and 2% over the value for the 1/8 in. square mesh elements. The Taylor series truncation error is also significantly reduced, further suggesting that it is truly insignificant. However, as the size of the mesh elements decreases, the number of finite difference equations increases exponentially. Comparing the 1/8 and 1/64 in. square mesh grids, the former results in 27,466 finite difference equations compared with 1,788,216 equations for the latter, while the computed torsion constant increases by only 2%. Excessive refinement of the finite difference mesh does not dramatically improve accuracy and imparts a significant computational penalty. Therefore, the mesh of 1/8 in. square elements used in this study provides a reasonable balance between solution accuracy and the number of finite difference equations that must be solved.

## Validation

The cross-section shape of modern precast concrete bridge girders can be idealized by building the shape from components that comprise squares, circular arcs, triangles, and rectangles. The software developed for this study was validated by computing the torsion constant for a square of side  $s$ , circle of diameter  $d$ , equilateral triangle of side  $s$ , and rectangles with width  $b$ , thickness  $t$ , and various depth-to-thickness ratios ( $b/t$  where  $t \ll b$ ). These shapes were chosen because of their close similarity to the components of a typical precast concrete girder cross section and because exact solutions are available for them. The square, circle, and equilateral triangle are modeled with a characteristic dimension ( $s$  or  $d$ ) of 10 in. (254 mm) for comparison with results reported by Eby et al. and Yoo. The width of the rectangles is modeled as 50 and 100 in. (1270 and 2540 mm) with a thickness of 5 in. (127 mm), resulting in aspect ratios of 10:1 and 20:1, respectively. This is roughly equivalent to the proportions of the wide top flange and web of the deepest sections evaluated.

The closed-form equations are as follows:

Square:  $J_e = \frac{9}{64}s^4$

Circle:  $J_e = \frac{\pi}{32}d^4$

Equilateral triangle:  $J_e = \frac{\sqrt{3}}{80}s^4$

Rectangle:<sup>14</sup>

$$J_e = \frac{bt^3}{3} \left[ 1 - \frac{192}{\pi^5} \left( \frac{t}{b} \right) \sum_{n=0,1,\dots} \frac{1}{(2n+1)^5} \tanh \frac{2n+1}{1} \pi \left( \frac{b}{t} \right) \right]$$

where

$J_e$  = exact torsion constant

$n$  = general ( $n^{\text{th}}$ ) term of a series

**Table 1** lists the torsion constant for the validation shapes based on a mesh with 1/8 in. (3.175 mm) square elements. The computer program produces very good results compared with the exact values.

As an additional measure of validation, the torsion constants for AASHTO Type I to Type VI sections are compared with those reported by Eby et al. and Yoo. The torsion constant is also estimated using AASHTO LRFD specifications Eq. (C4.6.2.2.1-1), for thin-walled open beams and Eq. (C4.6.2.2.1-2) for stocky open sections such as prestressed concrete I-beams. These equations are repeated here. Note that the nomenclature for  $J_1$  and  $J_2$  is used subsequently herein:

$$J_1 = \frac{1}{3} \sum bt^3 \quad (\text{AASHTO C4.6.2.2.1-1})$$

$$J_2 = \frac{A^4}{40.0I_p} \quad (\text{AASHTO C4.6.2.2.1-2})$$

where

$J_1$  = approximate torsion constant

$J_2$  = approximate torsion constant

$A$  = area of cross section

$I_p$  = polar moment of inertia

**Table 1.** Comparison of torsion constants of validation shapes with exact values and values published by others

Shape	$J_e$ , in. <sup>4</sup>	$J$ , in. <sup>4</sup> from this study	$J/J_e$	$J$ , in. <sup>4</sup> from Eby et al.	$J$ , in. <sup>4</sup> from Yoo
Square	1406	1405	0.99	1397	1405
Circle	982	954	0.97	n.d.	n.d.
Equilateral triangle	217	208	0.96	215	n.d.
Rectangle 10:1	1950	1950	1.0	n.d.	n.d.
Rectangle 20:1	4033	4033	1.0	n.d.	n.d.

Note:  $J$  = torsion constant;  $J_e$  = exact torsion constant; n.d. = no data. 1 in.<sup>4</sup> = 416,231 mm<sup>4</sup>.

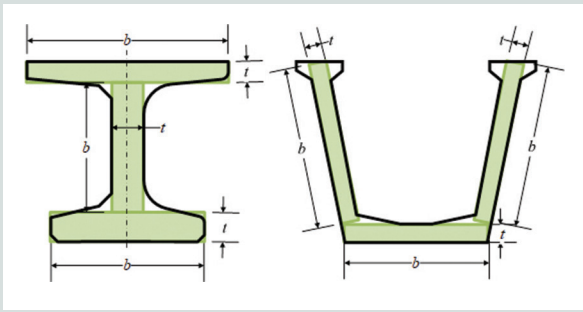


**Figure 4.** Discretization of typical precast concrete girder cross sections for use with the American Association of State Highway and Transportation Officials' *AASHTO LRFD Bridge Design Specifications* Eq. (C4.6.2.2.1-1) with left and right halves of I-beam section show chamfer and radius interior corners, respectively. Note:  $b$  = width of plate-like element;  $t$  = thickness of plate-like element.

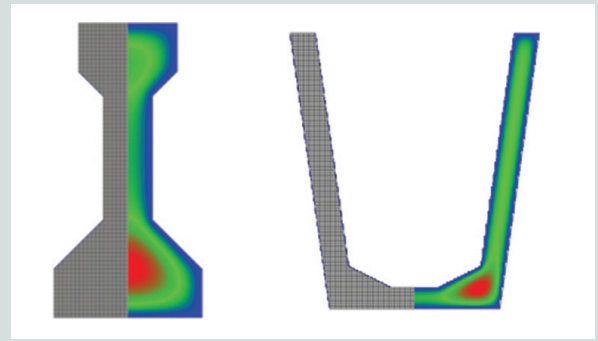


**Figure 5.** Finite difference mesh (left half of each section) and membrane ordinate contours (right half of each section) for American Association of State Highway and Transportation Officials Type II and Washington State Department of Transportation U78G4 girders using  $\frac{1}{8}$  in. square elements. Note: 1 in. = 25.4 mm.

**Figure 4** shows the discretization of typical girder sections for use with AASHTO LRFD specifications Eq. (C4.6.2.2.1-1). Flanges and webs were considered to be thin plates. The thickness of the discretized top and bottom flanges of I-beams were based on their average thickness, neglecting the interior corner chamfer or radius. The cross-sectional area of the discretized shape was generally slightly less than the actual area.

The AASHTO LRFD specifications commentary C4.6.2.1.1 states that Eq. (C4.6.2.2.1-2) substantially underestimates the torsion stiffness for some concrete I-beams and references Eby et al. for a more accurate solution. Yoo notes that torsion constants for AASHTO Type I to Type VI sections can deviate between 10% and 30% from the values found by more precise methods. This study found that the deviation can be more than 200% for some girder sections.

**Table 2** lists the torsion constants and compares  $J$  from

the AASHTO LRFD specifications equations with the values computed in this study. It is interesting to note that for the Type V section, AASHTO LRFD specifications Eq. (C4.6.2.2.1-2) gives a value of  $J$  that is 19% greater than the finite difference solution compared with the 29% increase reported by Yoo. This is to be expected due to the higher accuracy of the refined analysis used in this study.

Computational results were also validated by plotting three-dimensional membrane volumes (Fig. 1) and membrane ordinate contours (**Fig. 5**) and visually inspecting them for any obvious anomalies. Anomalies in the finite difference solutions were not observed.

Validation shows that the software computes torsion constants that were consistent with exact solutions and values computed by others. The successfully validated software was then used to compute torsion constants for modern precast concrete girders.

**Table 2.** Comparison of torsion constants for AASHTO girder section types with previously reported values and approximate values from the equations given in the *AASHTO LRFD Bridge Design Specifications*

AASHTO girder section types	$J$ , in. <sup>4</sup> from this study	$J$ , in. <sup>4</sup> from Eby et al.	$J$ , in. <sup>4</sup> from Yoo	$J_1$ , in. <sup>4</sup>	$J_1/J$ from this study	$J_2$ , in. <sup>4</sup>	$J_2/J$ from this study
Type I	4592	4745	4820	3755	0.82	5559	1.21
Type II	7621	7793	7372	6352	0.83	8231	1.08
Type III	16,734	17,044	16,210	13,731	0.82	17,803	1.06
Type IV	32,334	32,924	30,229	26,259	0.81	33,980	1.05
Type V	37,925	35,433	35,044	28,511	0.75	45,202	1.19
Type VI	39,461	36,071	37,347	30,047	0.76	43,584	1.10

Note: AASHTO = American Association of State Highway and Transportation Officials;  $J$  = torsion constant;  $J_1$  = approximate torsion constant computed with *AASHTO LRFD Bridge Design Specifications* Eq. (C4.6.2.2.1-1);  $J_2$  = approximate torsion constant computed with *AASHTO LRFD Bridge Design Specifications* Eq. (C4.6.2.2.1-2). 1 in.<sup>4</sup> = 416,231 mm<sup>4</sup>.

**Table 3.** Torsion constant evaluation for sampling of girder sections considered in this study

Name	Agency	$A_{mesh}$ , in. <sup>2</sup>	$A$ , in. <sup>2</sup>	$A_{mesh}/A$	$J$ , in. <sup>4</sup>	$J_1$ , in. <sup>4</sup>	$J_1/J$	$J_2$ , in. <sup>4</sup>	$J_2/J$
Type I	AASHTO	275.0	276.0	0.996	4592	3996	0.87	5559	1.21
CBT 30	Colorado DOT	738.9	739.8	0.999	18,607	11,375	0.61	43,089	2.32
Tx34	Texas DOT	626.6	627.3	0.999	17,660	11,528	0.65	29,991	1.70
FIB 36	Florida DOT	805.8	806.6	0.999	30,342	19,365	0.64	50,721	1.67
WF36G	Washington DOT	688.5	690.8	0.997	13,997	8467	0.60	29,034	2.07
WF120	California DOT	1352.9	1353.2	1.000	33,638	23,787	0.71	30,687	0.91
CBT 90	Colorado DOT	1158.9	1159.8	0.999	25,452	18,235	0.72	31,988	1.26
FIB 96	Florida DOT	1225.8	1226.6	0.999	37,190	26,225	0.71	35,417	0.95
NU2000	Nebraska DOT	909.7	903.1	1.007	17,165	12,175	0.71	19,536	1.14
WF100G	Washington DOT	1072.5	1082.8	0.990	18,602	13,369	0.72	21,512	1.16

Note:  $A$  = area of cross section;  $A_{mesh}$  = area of cross section of finite difference mesh; AASHTO = American Association of State Highway and Transportation Officials; DOT = department of transportation;  $J$  = torsion constant;  $J_1$  = approximate torsion constant computed with AASHTO LRFD Bridge Design Specifications Eq. (C4.6.2.2.1-1);  $J_2$  = approximate torsion constant computed with AASHTO LRFD Bridge Design Specifications Eq. (C4.6.2.2.1-2). 1 in.<sup>2</sup> = 645.2 mm<sup>2</sup>; 1 in.<sup>4</sup> = 416,231 mm<sup>4</sup>.

## Torsion constants for modern precast concrete girders

The software program developed for this study was used to compute the torsion constant for 167 different modern precast concrete bridge girder sections that are commonly used in the United States. **Table 3** lists girder type, agency, cross-sectional area of the element mesh, cross-sectional area of the girder section, ratio of the mesh area to the area of the girder, torsion constant computed using the refined method of this study and by the AASHTO LRFD specifications approximate equations, and ratios of the approximate to refined values of  $J$  for a sampling of the girder sections studied. The finite difference mesh accounts for 99% to 100% of the cross-sectional area of the girder section, indicating that the simple square mesh approximation, with 1/8 in. (3.175 mm) square mesh elements, sufficiently models the girder section. **Figure 6** shows the ratio of the approximate to refined values of  $J$  for all girder sections considered in this study as a function of the overall height-to-width ratio of the section. This figure shows clearly that AASHTO LRFD specifications Eq. (C4.6.2.2.1-1) consistently underestimates and Eq. (C4.6.2.2.1-2) overestimates the torsion constant for sections with a height-to-width ratio less than about 2.0 to 2.5. Estimates by these equations ranged from 36% less than to 230% more than the torsion constant computed by the refined analysis used in this study.

Figures 1 and 5 illustrate that for short, stocky I-beams, such as the AASHTO Type II section, the membrane volume is hemispherical in nature in the web-bottom flange region. The use of AASHTO LRFD specifications Eq. (C4.6.2.2.1-1) approximates this region as a rectangle, which oversimplifies the behavior in the region and contributes to the underestimation found in this study.

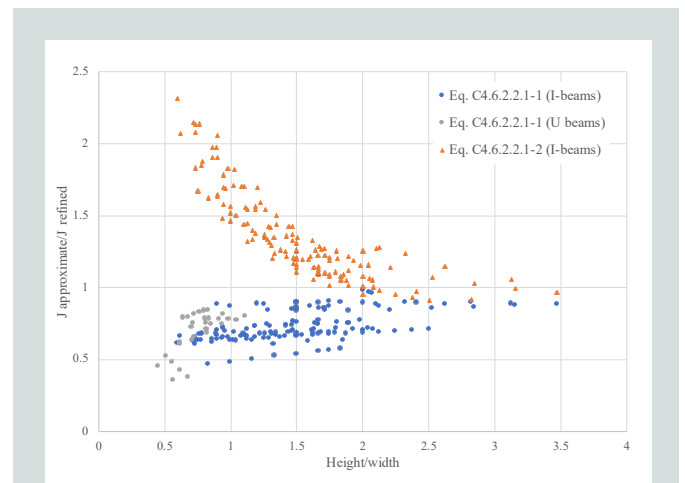


**Figure 6.** Ratio of the American Association of State Highway and Transportation Officials' AASHTO LRFD Bridge Design Specifications approximate torsion constant to refined torsion constant computed in this study for all height-to-width ratios of the girder sections considered. Note:  $J$  approximate = approximate torsion constant;  $J$  refined = refined torsion constant.

Eby et al. note that the equation adopted as AASHTO LRFD specifications Eq. (C4.6.2.2.1-2) is not applicable to sections with reentrant corners unless the section is subdivided into smaller areas not containing reentrant corners. The idealized I-beams used in this study, as well as in the study by Eby et al., all have reentrant corners at the web-flange interfaces. AASHTO does not make this distinction, which contributes to the overestimate.

The online appendix, which is available at <http://pci.org/2021-May-Appx>, provides an extensive catalog of geometric

properties for the girder sections considered in this study. The minor axis moment of inertia for precast concrete girders is infrequently reported by agencies. This is a key parameter in lateral girder stability analysis and is listed in the appendix.

## Conclusion

Using modern digital computing technology and advanced parallel programming constructs, the Prandtl membrane analogy has been successfully evaluated using the finite difference method, resulting in accurate torsion constants for many precast concrete bridge girders used in the United States. The AASHTO LRFD specifications approximate equations were evaluated and compared with the more precise finite difference solution. The approximation for thin-walled open beams (AASHTO LRFD specifications Eq. [C4.6.2.2.1-1]) consistently underestimated the torsion constant. Yoo's assertion that the approximate formula given in AASHTO LRFD specifications Eq. (C4.6.2.2.1-2) for stocky open sections does not yield reasonably accurate results for AASHTO Type I to Type VI girder sections was confirmed. Furthermore, this study shows that the approximation, in general, does not provide reasonably accurate results for modern girder sections.

This study provides an extensive catalog of precast concrete girder section properties. The catalog includes the Saint-Venant torsion constants, which have not been previously published. The authors encourage owner agencies and industry organizations to adopt the torsion constants reported in this study and to incorporate them into bridge design manuals and other appropriate reference materials.

## References

1. Seguirant, S. J. 1998. "New Deep WSDOT Standard Sections Extend Spans of Prestressed Concrete Girders." *PCI Journal* 43 (4): 92–119.
2. Geren, K. L., and M. K. Tadros. 1994. "The NU Precast/Prestressed Concrete Bridge I-Girder Series." *PCI Journal* 39 (3): 26–39.
3. Riechers, K. 2015. "Illinois Girder Shapes Offer Design Flexibility." *Aspire* 9 (4): 28–29.
4. Hass, R., and A. Ehrlich. 2019. "Minnesota's MH Shape: The Development of Efficient Shallow-Depth Prestressed Concrete Beams." *Aspire* 13 (3): 34–35.
5. AASHTO (American Association of State Highway and Transportation Officials). 2017. *AASHTO LRFD Bridge Design Specifications*. 8th ed. Washington, DC: AASHTO.
6. Boresi, A. P., and K. P. Chong. 1987. *Elasticity in Engineering Mechanics*. New York, NY: Elsevier Science Publishing Co. Inc.

7. PCI Bridge Committee. 2016. *Recommended Practice for Lateral Stability of Precast, Prestressed Concrete Bridge Girders*. CB-02-16. Chicago, IL: PCI.
8. Eby, C. C., J. M. Kulicki, C. N. Kostem, and M. A. Zelin. 1973. "Evaluation of St. Venant Torsional Constants for Prestressed Concrete I-Beams." Fritz Laboratory report 400.12. Department of Civil Engineering, Lehigh University, Bethlehem, PA.
9. Yoo, C. H. 2000. "Torsional and Other Properties of Prestressed Concrete Sections." *PCI Journal* 45 (3): 66–72.
10. PCI Bridge Design Manual Steering Committee. 2011. *PCI Bridge Design Manual*. MNL-133. 3rd ed. Chicago, IL: PCI.
11. Bonanno, F. R. 1958. "Torsion Constants of Certain Cross-Sections by Non-Topographic Photogrammetry." *Photogrammetric Engineering* 24 (5): 803–809.
12. Burden, R. L., and J. D. Faires. 1989. *Numerical Analysis*. 4th edition. Boston, MA: PWS-KENT Publishing Co.
13. Causon, D. M., and C. G. Mingham. 2010. *Introductory Finite Difference Methods for PDEs*. Ventus Publishing ApS.
14. Connor, J. J., 1976. *Analysis of Structural Member Systems*. New York, NY: Ronald Press.

## Notation

$A$	= area of cross section
$A_{mesh}$	= area of cross section of finite difference mesh
$b$	= width of plate element
$d$	= diameter
$G$	= shear modulus
$I_p$	= polar moment of inertia
$J$	= torsion constant
$J_{approximate}$	= approximate torsion constant
$J_e$	= exact torsion constant
$J_{refined}$	= refined torsion constant
$J_1$	= approximate torsion constant computed with American Association of State Highway and Transportation Officials' <i>AASHTO LRFD Bridge Design Specifications</i> Eq. (C4.6.2.2.1-1)

$J_2$  = approximate torsion constant computed with American Association of State Highway and Transportation Officials' *AASHTO LRFD Bridge Design Specifications* Eq. (C4.6.2.2.1-2)

$L$  = member length

$n$  = general ( $n^{\text{th}}$ ) term of a series

$N$  = number of finite difference mesh points

$s$  = side of square or equilateral triangle

$t$  = thickness of plate-like element

$T$  = torque

$\theta$  = angle of twist



## About the authors



Richard Brice, PE, is the Bridge Design Technology Unit manager for the Bridge and Structures Office at the Washington State Department of Transportation in Olympia, Wash.



Richard Pickings, PE, is president of BridgeSight Inc., a leading bridge engineering software company in South Lake Tahoe, Calif.

## Abstract

Many bridge owners have developed new precast, prestressed concrete bridge girder sections that are optimized for high-performance concrete and pretensioning strands with diameters greater than 0.5 in. (12.7 mm). Girder sections have been developed for increased span capacities, while others fill a need in shorter span ranges.

Accurate geometric properties are essential for design. Common properties, including cross-sectional area, location of centroid, and major axis moment of inertia, are generally easy to compute and are readily available in standard design references. Computation of the torsion constant is a different matter. This paper presents the methods and results of a study to determine the torsion constant for many of the modern precast, prestressed concrete bridge girders used in the United States and compares the results with values from the approximate methods of the AASHTO LRFD specifications.

## Keywords

Bridge, finite difference mesh, girder, torsion constant.

## Review policy

This paper was reviewed in accordance with the Precast/Prestressed Concrete Institute's peer-review process.

## Reader comments

Please address any reader comments to *PCI Journal* editor-in-chief Tom Klemens at [tklemens@pci.org](mailto:tklemens@pci.org) or Precast/Prestressed Concrete Institute, c/o *PCI Journal*, 8770 W. Bryn Mawr Ave., Suite 1150, Chicago, IL 60631. [f](#)